Coupled surface polaritons and the Casimir force

Carsten Henkel, Karl Joulain, Jean-Philippe Mulet, Jean-Jacques Greffet

▶ **To cite this version:**

Carsten Henkel, Karl Joulain, Jean-Philippe Mulet, Jean-Jacques Greffet. Coupled surface polaritons and the Casimir force. 2003. hal-00000557v3

HAL Id: hal-00000557

https://hal.science/hal-00000557v3

Preprint submitted on 7 Nov 2003

HAL is a multi-disciplinary open access archive for the deposit and dissemination of scientific research documents, whether they are published or not. The documents may come from teaching and research institutions in France or abroad, or from public or private research centers.

L'archive ouverte pluridisciplinaire **HAL**, est destinée au dépôt et à la diffusion de documents scientifiques de niveau recherche, publiés ou non, émanant des établissements d'enseignement et de recherche français ou étrangers, des laboratoires publics ou privés.

Coupled surface polaritons and the Casimir force

C. Henkel*
Institut für Physik, Universität Potsdam, Am Neuen Palais 10, 14469 Potsdam, Germany

K. Joulain,† J.-Ph. Mulet,‡ and J.-J. Greffet
Laboratoire EM2C, Ecole Centrale Paris, 92295 Châtenay-Malabry CEDEX, France
(Dated: 06 November 2003)

The Casimir force between metallic plates made of realistic materials is evaluated for distances in the nanometer range. A spectrum over real frequencies is introduced and shows narrow peaks due to surface resonances (plasmon polaritons or phonon polaritons) that are coupled across the vacuum gap. We demonstrate that the Casimir force originates from the attraction (repulsion) due to the corresponding symmetric (antisymmetric) eigenmodes, respectively. This picture is used to derive a simple analytical estimate of the Casimir force at short distances. We recover the result known for Drude metals without absorption and compute the correction for weakly absorbing materials.

PACS numbers: 42.50.Pq, 42.50.Lc, 73.20.Mf

ccsd-00000557 (version 3) : 7 Nov 2003

I. INTRODUCTION

Van der Waals and Casimir forces are among the few macroscopic manifestations of vacuum fluctuations. Since the seminal paper by Casimir [1] showing the existence of an attraction between two perfect conductors separated by a vacuum gap, an abundant literature has been devoted to this effect. In particular, the relevance of retardation, finite conductivity, and finite temperature have been studied (see, e.g., [2]). Exhaustive lists of references can be found in several review papers such as [3, 4, 5].

In the last five years, the interest in Casimir forces has increased due to the existence of new measurements with improved accuracy [6, 7]. This has challenged theoreticians to quantify the corrections to the ideal case (zero temperature, perfect conductors, flat interfaces) that must be taken into account for an accurate comparison with experiments [8, 9, 10, 11, 12, 13]. Furthermore, the developments of micro-electromechanical systems (MEMS), for example, have shown that the Casimir effect is becoming an issue in nano-engineering [14, 15]. Indeed, these short-range forces could seriously disturb the performances of MEMS [16].

From a theoretical point of view, different methods exist to calculate Casimir forces. Casimir himself [1] determined the electromagnetic eigenfrequencies of the system and summed them in order to obtain the system's zero-point energy. The force is found by differentiation of this energy with respect to the geometrical distance separating the bodies [1, 17]. Ingenious subtraction procedures are often required to obtain a finite value for the Casimir energy, and realistic dispersive or absorbing materials can be dealt with using contour integrals over complex frequencies [18]. Another method, used by Lifshitz [19], considers fluctuating currents driven by thermal or vacuum fluctuations in the whole space. These currents, whose spatial correlations are known through the fluctuation dissipation theorem, interact via the electromagnetic fields they radiate. The force is obtained by calculating the flux of the Maxwell stress tensor across a surface separating the bodies. One thus gets an integral over all possible partial wave contributions. For two parallel plates separated by a vacuum gap, for example, the partial waves can be labelled by their frequency, wave vector parallel to the interface, and polarization. By using clever contour deformation, Lifshitz greatly simplified the calculation of the Casimir force integral. The principal drawback of this approach is that the integrand can no longer be interpreted as a force spectrum.

In this paper, we use an alternative approach and study the force integral over real frequencies and wave vectors. We show for generic materials (semiconductors and real metals) that in the near-field regime (separation distance small compared to the wavelengths considered), the frequency spectrum of the force exhibits peaks located close to surface-polariton frequencies. These peaks give the essential contribution to the Casimir force in this regime. We identify two types of resonant surface modes, binding and antibinding, that contribute respectively with an attractive and a repulsive term to the force. This substantiates early suggestions [20, 21] that the Casimir force is due to surface modes, see also the recent papers by Genet et al. [13, 22].

We finally focus on materials whose dielectric function is modeled by a Lorentzian resonance, including a nonzero absorption. We are able to use the qualitative suggestions mentioned above and propose a quantitative estimation of the Casimir force in terms of coupled surface resonances. The dominant contribution of these resonances at nanometer distances allows to perform exactly the integral over the mode frequencies, whereas the integral over the wave vector is computed to first order in the absorption. We show that the respective contributions of binding/antibinding modes give a simple and accurate analytical estimate for the short-distance Casimir force, recovering previous results for nonabsorbing Drude materials [10]. In the corresponding Hamaker constant, we in-

*Electronic address: Carsten.Henkel@quantum.physik.uni-potsdam.de
†Currently at Laboratoire d'études thermiques, ENSMA, 86960 Futuroscope Cedex, France.
‡Currently at The Institute of Optics, University of Rochester, Rochester NY 14627, USA.

clude corrections due to material losses. The accuracy of our results is established by comparing to numerical evaluations of Lifshitz theory, using tabulated data for the dielectric functions [23]. The paper concludes with a discussion of possibilities to "tune" the Casimir force that are suggested by our approach.

II. SURFACE RESONANCES IN THE FREQUENCY SPECTRUM

The starting point for our calculation of the Casimir force is Rytov's theory of fluctuating electrodynamics in absorbing media [24] that has been used by Lifshitz in his seminal paper [19]. This scheme applies to dispersive or absorbing materials, as long as their dielectric response is linear. It has also been shown to provide a suitable framework for a consistent quantization procedure of the macroscopic Maxwell equations (see [25, 26] and references therein).

In the following, we focus on the standard geometry of two planar half-spaces made from identical material (of local complex dielectric constant $\varepsilon(\omega)$) and separated by a vacuum gap of width d. In the Rytov-Lifshitz method, the Casimir force is computed from the expectation value of the Maxwell stress tensor at an arbitary position in the gap. At zero temperature and after subtraction of divergent contributions, Lifshitz gets a force per unit area given by [19]

$$F = \int_0^\infty \frac{\mathrm{d}\omega}{2\pi} \int_0^\infty \frac{\mathrm{d}u}{2\pi}\, F(u,\omega) \tag{1}$$

$$F(u,\omega) = \frac{2\hbar\omega^3 u}{c^3}\,\mathrm{Im}\left(v \sum_{\mu\,=\,\mathrm{s,\,p}} \frac{r_\mu^2(u,\omega)\,\mathrm{e}^{-2\omega v d}}{1 - r_\mu^2(u,\omega)\,\mathrm{e}^{-2\omega v d/c}} \right), \tag{2}$$

where $v = (u^2-1)^{1/2}$ ($\mathrm{Im}\, v \le 0$), and r_μ is the Fresnel reflection coefficient for a plane wave with polarization μ and wavevector $K = \omega u/c$ parallel to the vacuum-medium interface. We use the convention that an attractive force corresponds to $F > 0$. We note that Rytov's approach allows for an easy generalization to different media held at different nonzero temperatures. The radiation force on a small polarizable sphere above a heated surface has been discussed previously in [27]. Results for the non-equilibrium Casimir force will be reported elsewhere.

Lifshitz evaluated the integrals (1) by deforming integration contour in the complex plane to arrive at an integral over imaginary frequencies $\omega = \mathrm{i}\xi$. The integration then requires the continuation of the dielectric function from real-frequency data to $\varepsilon(\mathrm{i}\xi)$, using analyticity properties as discussed in [9, 10]. We follow here a different route and continue to work with real ω and u, taking advantage of the fact that Lifshitz' results provides us with an expression for the frequency spectrum $F(\omega) = \int F(u,\omega) du/2\pi$ of the Casimir force. Note that the force spectrum is more difficult to define in a calculation based on mode summation, see, e.g., [28, 29].

For a polar material like SiC, the spectrum of the force is dominated by narrow peaks in the UV and in the IR (Fig. 1) when the distance d is reduced to the nanometer range. These peaks can be ascribed to the surface phonon polaritons in the IR and to surface plasmon polaritons (SPP) in the UV. The largest contribution comes from the UV surface plasmon polariton even though larger losses make it broader. The large difference between the UV and the IR contributions in Fig. 1 is due to the factor ω^3 in Eq. (2). In Fig. 2, we plot the spectrum of the force between two aluminum half-spaces, using tabulated data for the dielectric function [23]. The dominant contribution to the force is clearly due to the surface plasmon polaritons. Indeed, the frequency of the peaks corresponds to the frequency Ω of the asymptote of the SPP dispersion rela-

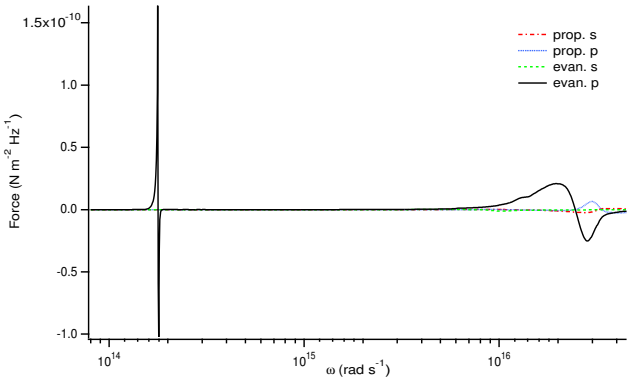

FIG. 1: Contributions of s and p polarized, propagating and evanescent modes to the force spectrum (Eq. (2) integrated over the wavevector u). Distance $d = 10$ nm. Material: SiC, dielectric function taken from tabulated data [23]. The corresponding surface resonances ($\mathrm{Re}\,\varepsilon(\omega) = -1$) are located at $1.78 \times 10^{14}\ \mathrm{s}^{-1}$ in the IR and $2.45 \times 10^{16}\ \mathrm{s}^{-1}$ in the UV.

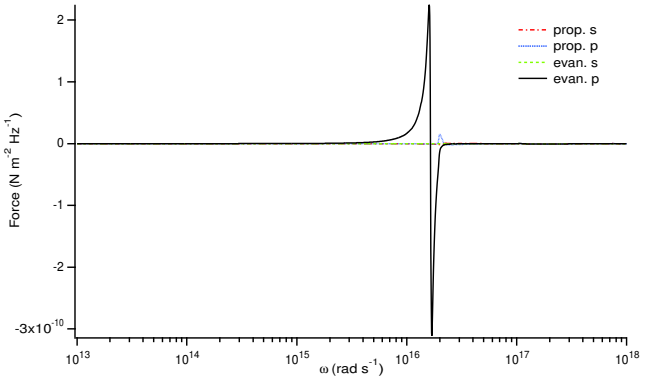

FIG. 2: Contributions of s and p polarized, propagating and evanescent modes to the force spectrum (Eq. (2) integrated over the wavevector u). Distance $d = 10$ nm. Material: aluminum, described by tabulated optical data [23].

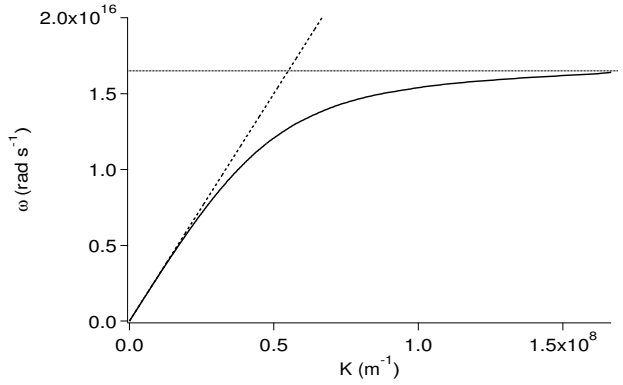

FIG. 3: Dispersion relation [Eq. (3)] of the surface plasmon polariton on a flat interface vacuum/aluminum. The dielectric function is taken from the data tabulated in [23]. We plot the real part of ω versus the real part of the parallel wavevector $K = u\omega/c$.

tion [30] (see Fig. 3)

$$u_{\rm SPP} = \sqrt{\frac{\varepsilon(\omega)}{\varepsilon(\omega)+1}}, \tag{3}$$

where the sign of the square root is chosen such that $\mathrm{Re}\, u_{\rm SPP} > 1$. It is seen in Eq. (3) that the frequency Ω is given by the condition $\mathrm{Re}\,\varepsilon(\Omega) = -1$. This corresponds to a large increase of the density of states and therefore to a peak in the energy density [31, 32]. The polarization dependence of the force spectrum provides a second argument in favor of a surface plasmon polariton. In Figs. 1, 2, we have separated the contributions to the spectrum according to the mode polarization (s or p). The modes in the cavity can further be classified into evanescent (surface) modes ($u > 1$) and propagating (guided) modes ($0 \leq u \leq 1$). Among the four contributions it is seen that the leading one comes from the p-polarized surface modes, of which the SPP is a special case.

It is worthwhile pointing out that for a perfectly conducting metal, the spectrum of the force would be completely different because of the lack of SPP. The usual picture of the Casimir effect in that case is based on the modified density of states for propagating waves between the two plates. This picture includes only what we have called guided modes and ignores surface (or evanescent) modes.

We observe from Figs.1,2 that the contribution of the force is either positive or negative depending on the frequency. We analyze this behaviour in the next section.

III. BINDING AND ANTIBINDING RESONANCES

In order to further analyze the role of SPPs for the Casimir force, we plot in Fig. 4a the integrand $F(u,\omega)$ as given by Eq. (2) for two aluminum half-spaces separated by a distance of $d = 10$ nm. Two branches emerge with dominant contributions, the higher-frequency branch yielding a negative contribution whereas the lower branch gives a positive (attractive)

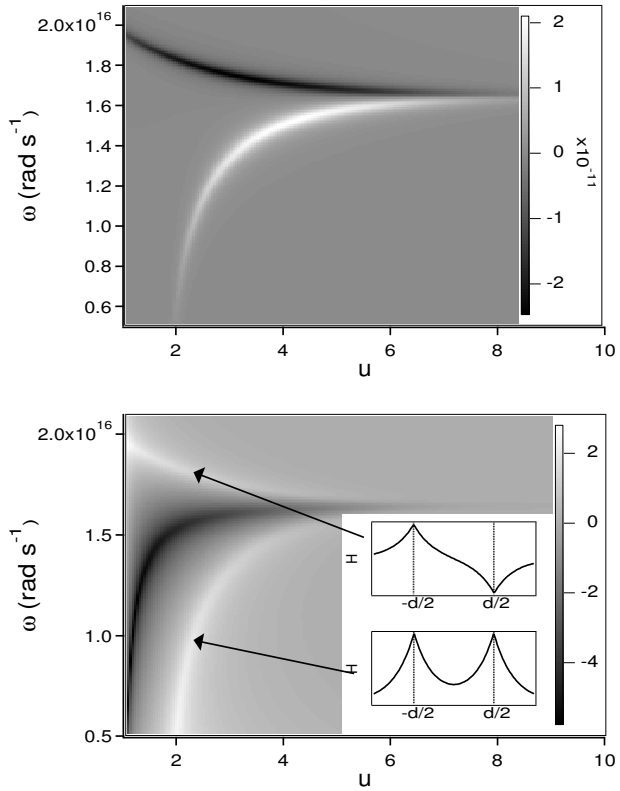

FIG. 4: (a) Wavevector resolved spectrum of the Casimir force [Eq. (2)] in the (u,ω) plane between two aluminum half spaces separated by a distance of 10 nm. The frequency of the flat asymptote corresponds to the peaks of the force spectrum Fig. 2. Light (dark) areas: attractive (repulsive) force. (b) Resonant denominator $1/|1 - r_{\rm p}^2\, {\rm e}^{-2\omega v d/c}|^2$ in the (u,ω) plane, the grayscale giving the logarithm to base 10. The dispersion relation of the coupled surface resonance corresponds to the light areas; dark area: dispersion relation for a single interface [Eq. (3)]. Dielectric function extracted from tabulated data [23]. The inset sketches the magnetic field of the coupled surface resonances (antisymmetric and symmetric combinations).

contribution. These two branches are reminiscent of the dispersion relation of a SPP on a two interfaces system. It is given by the complex poles of the reflection factor of the two interfaces system in the (u,ω) plane:

$$1 - r_{\rm p}^2\, {\rm e}^{-2\omega v d/c} = 0 \tag{4}$$

In order to illustrate the influence of the SPP dispersion relation on the force, we plot in Fig. 4b the quantity $1/|1 - r_{\rm p}^2\, {\rm e}^{-2\omega v d/c}|^2$ in the real (u,ω) plane. Comparing Figs. 4b and 4a, it is clearly seen that the main contribution to the force is due to the SPP. In addition, we observe on Fig. 4b a dark line which corresponds to minima of $1/|1 - r_{\rm p}^2\, {\rm e}^{-2\omega v d/c}|^2$. This can be attributed to very large values of the reflection factor $r_{\rm p}$. Thus, the dark line is the dispersion relation of the SPP on a single flat interface. Note that the Casimir force shows no prominent feature in this region.

In Fig. 5, we plot the force for a spacing $d = 100$ nm: the two branches tend to merge with the flat interface dispersion

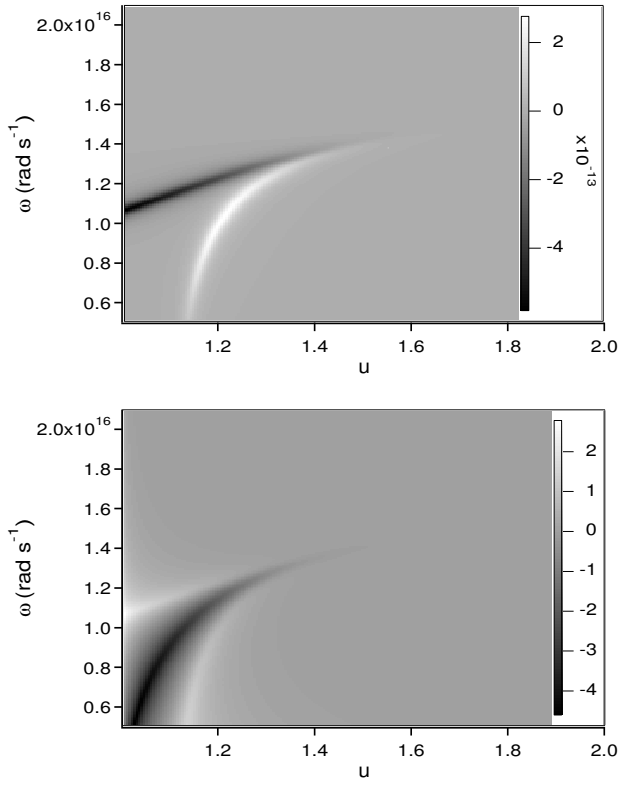

FIG. 5: Same as Fig.4, but for a separation $d = 100\,\mathrm{nm}$.

relation. The following interpretation thus emerges: when the surfaces approach each other, the overlapping of the two SPP leads to a splitting of the polariton frequencies [33, 34]. The frequency splitting can be found from the solutions of Eq. (4) which are implicitly defined by (see also [22])

$$r_{\mathrm{p}}(u,\omega) = \pm \mathrm{e}^{\omega v d/c}. \tag{5}$$

The signs correspond to either symmetric or antisymmetric mode functions (for the magnetic field), as shown in Appendix A and sketched in Fig. 4b. The symmetric (antisymmetric) branch corresponds to a lower (higher) resonance frequency, respectively, similar to molecular orbitals and tunneling doublets [35]. These branches contribute with opposite signs to the Casimir force, due to the identity

$$\begin{aligned} &\frac{2\, r_{\mathrm{p}}^2(\omega,u)\, \mathrm{e}^{-2\omega v d}}{1 - r_{\mathrm{p}}^2(\omega,u)\, \mathrm{e}^{-2\omega v d}} = \\ &\frac{r_{\mathrm{p}}(\omega,u)\, \mathrm{e}^{-\omega v d}}{1 - r_{\mathrm{p}}(\omega,u)\, \mathrm{e}^{-\omega v d}} - \frac{r_{\mathrm{p}}(\omega,u)\, \mathrm{e}^{-\omega v d}}{1 + r_{\mathrm{p}}(\omega,u)\, \mathrm{e}^{-\omega v d}}, \end{aligned} \tag{6}$$

where the first (second) term is peaked at the symmetric (antisymmetric) cavity mode. The symmetry of the resonance mode function hence determines the attractive or repulsive character of its contribution to the Casimir force. We show in Appendix A by evaluating explicitly the Maxwell stress tensor, that *symmetric modes are binding* as in molecular physics.

We note that the splitting in Eq. (6) of the force spectrum gives meaningful results also after integration because for evanescent waves, both terms converge separately. We also point out that for a complex permittivity $\varepsilon(\omega)$ (as required by the Kramers-Kronig relations for a dispersive material), the SPP dispersion relation necessarily moves into the complex plane and is never satisfied in the real (u,ω)-plane, thus excluding any singularities of the integral (1).

IV. SHORT-DISTANCE LIMIT

The short-distance behaviour of the Casimir force between non-perfect metals has been computed in [9, 10] using tabulated data for the dielectric function and integrating over imaginary frequencies. We show here that these results can also be recovered with a real frequency calculation. In particular, we prove that the interaction between SPPs across the vacuum gap quantitatively accounts for the short-distance Casimir force derived in [10], thus completing qualitative discussions put forward by Gerlach [21] and Genet, Lambrecht, and Reynaud [22].

For definiteness, let us adopt a Lorentz-Drude model for the dielectric function

$$\varepsilon(\omega) = 1 + \frac{2(\Omega^2 - \omega_0^2)}{\omega_0^2 - \mathrm{i}\gamma\omega - \omega^2}, \tag{7}$$

with resonance frequency ω_0 and damping coefficient γ. The corresponding plasma frequency is $[2(\Omega^2 - \omega_0^2]^{1/2}$. With this convention, the large u asymptote of the SPP dispersion (3) occurs at $\omega \approx \Omega$. This model can be used to describe either dielectrics or metals when $\omega_0 = 0$. In the region of large wavevectors, the p-polarized reflection coefficient has a pole at Ω:

$$u \gg 1: \quad r_{\mathrm{p}}(\omega,u) \approx \frac{\varepsilon(\omega)-1}{\varepsilon(\omega)+1} = \frac{\Omega^2 - \omega_0^2}{\Omega^2 - \mathrm{i}\gamma\omega - \omega^2}. \tag{8}$$

From Figs.1, 2, we know that the force is significant only in a range around the SPP resonance. It follows that the model for $\varepsilon(\omega)$ is needed only in this limited range. We have checked that Eq. 8 with $\omega_0 = 0$ is well suited to describe the reflection data computed from tabulated data for aluminum. Note that the results of the fitted parameters (Ω and γ are indicated in the caption of fig.4) differ from the usual bulk plasma frequency and damping rates that we would get from a fit over the entire spectrum.

We have checked that this formula is well suited to describe the reflection coefficient computed from tabulated optical data in the frequency region around the SPP resonance. For aluminum, we get a good agreement with the values given in the caption of Fig.6. These values do not correspond, of course, to the usual bulk plasma frequency and damping rates that enter in the Drude model of the dielectric function at low frequencies.

With this form of the reflection coefficient, Eq. (5) yields the following dispersion relation for the (anti)symmetric SPP resonances, neglecting for the moment the damping coefficient γ:

$$\omega_{\pm}^2 \approx \Omega^2 \left(1 \mp \mathrm{e}^{-\omega_{\pm} u d/c}\right). \tag{9}$$

We have used $v \approx u$ for $u \gg 1$. For large u, we solve by iteration and find that $\omega_\pm \lessgtr \Omega$. As announced above, the symmetric mode (upper sign) occurs at a lower resonance frequency.

To derive an analytical estimate for the Casimir force, we retain in Eq. (2) only the contribution of p-polarized, evanescent waves, containing the SPP resonance. Introducing the new variable $x = \omega v d/c$, we get using the identity (6)

$$F = \frac{\hbar}{4\pi^2 d^3} \operatorname{Im} \int_0^\infty \mathrm{d}\omega \int_0^\infty x^2 \mathrm{d}x \times \sum_{\lambda=\pm 1} \frac{\lambda\, \mathrm{e}^{-x}}{r_\mathrm{p}^{-1}(\omega, cx/(\omega d)) - \lambda\, \mathrm{e}^{-x}}, \qquad (10)$$

where $\lambda = \pm 1$ corresponds to symmetric (antisymmetric) modes, respectively. The integral is dominated by the range $x \sim 1$ and $\omega \sim \Omega$. To leading order in $\Omega d/c \to 0$, we can thus use the asymptotic form of r_p valid for large u given by Eq. (8). Performing the integral over ω analytically and including damping to first order in γ/Ω yields

$$F = \frac{\hbar\Omega}{4\pi\, d^3} \int_0^\infty \mathrm{d}x\, x^2 \times \sum_{\lambda=\pm 1} \left(\frac{\lambda z\, \mathrm{e}^{-x}}{2\sqrt{1-\lambda z\, \mathrm{e}^{-x}}} - \frac{\gamma \lambda z\, \mathrm{e}^{-x}}{2\pi\Omega(1-\lambda z\, \mathrm{e}^{-x})} \right) \qquad (11)$$

where $z = 1 - \omega_0^2/\Omega^2$. This result shows clearly that symmetric and antisymmetric modes give Casimir forces of opposite sign. The first term in the parenthesis can be computed by expanding the square root in a power series in $\lambda z\, \mathrm{e}^{-x}$, leading to an infinite series given in [10, 22]. The second term, the correction due to damping, can be integrated in terms of the polylogarithmic function, so that we finally have

$$F = \frac{\hbar\Omega}{4\pi d^3} \left(\alpha(z) - \frac{\gamma\, \mathrm{Li}_3(z^2)}{4\pi\Omega} \right), \qquad (12)$$

where

$$\alpha(z) = \frac{1}{4} \sum_{n=1}^\infty z^{2n} \frac{(4n-3)!!}{n^3 (4n-2)!!} \qquad (13)$$

and

$$\mathrm{Li}_3(z^2) = \sum_{n=1}^\infty \frac{z^{2n}}{n^3}. \qquad (14)$$

For completeness, we give the asymptotic series for small ω_0/Ω ($z \to 1$)

$$\alpha(z) \approx 0.1388 - 0.32\,(1-z) + 0.4\,(1-z)^2 \qquad (15)$$

$$\mathrm{Li}_3(z^2) \approx \zeta(3) - \frac{\pi^2}{3}(1-z) + \left[3 - \frac{\pi^2}{6} - 2\log(2(1-z)) \right] (1-z)^2 \qquad (16)$$

with $\zeta(3) \approx 1.202$. (The coefficient of the second order term in Eq. (15) is only accurate up to a logarithmic correction.)

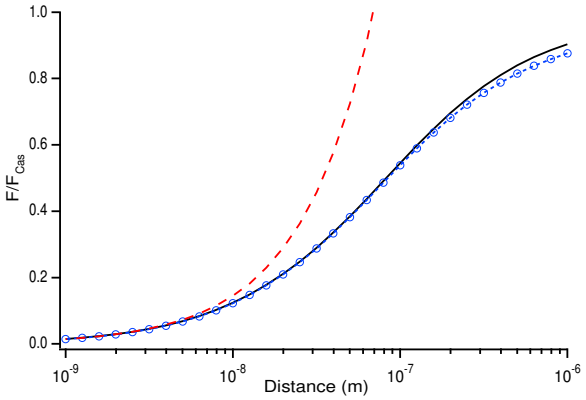

FIG. 6: Comparison of different expressions for the Casimir force between aluminum surfaces. We plot the ratio $F(d)/F_\mathrm{Cas}(d)$ where $F_\mathrm{Cas}(d) = \hbar c \pi^2/(240 d^4)$ is the Casimir force for perfect mirrors. Solid line: numerical integration of Eq. (2), using tabulated optical data [23, 36]. Short-dashed line with circles: same with a model dielectric function of Drude form [Eq. (7)] with $\omega_0 = 0$, $\Omega = 1.66 \times 10^{16}\ \mathrm{s}^{-1}$, and $\gamma/\Omega = 0.036$. These parameters have been obtained from a plot of the reflection coefficient $(\varepsilon(\omega)-1)/(\varepsilon(\omega)+1)$ based on the tabulated data that has been fitted to the form given in Eq. (8). Long-dashed line: short-distance asymptotics (12) with the same values for ω_0, Ω, γ.

Our result Eq. (12) for the short-distance Casimir force agrees with the formula given in [10, 22] in the special case $\gamma = 0$, $\omega_0 = 0$ (lossless Drude model). A very similar expression has been found in [26]. We compare Eq. (12) in Fig. 6 to the full integral Eq. (2) for the case of aluminum: it turns out to be quite accurate for distances $d \leq 0.1\,\lambda_\mathrm{SPP}$ where $\lambda_\mathrm{SPP} = 115$ nm is the wavelength of the SPP with the largest frequency [36]. In the case of aluminum, the first order correction in γ/Ω is 2.5% of the zeroth order value of the force. The plot also shows that for the numerical integration, the tabulated data and the Lorentz-Drude model (7) with parameters fitted around the surface resonance give very close results over a large range of distances. This is another indication that the short-range Casimir force between real metals is dominated by a narrow frequency range. Differences of the order of a few percent appear at large distances where the Casimir force is dominated by the low-frequency behaviour of the reflection coefficient that is not accurately modelled with the fitted parameters.

We finally note that the correction of order γ/Ω derived here introduces the effects of losses and must not be confused with the correction due to a finite real permittivity This is already taken into account by the finite value of the plasma frequency Ω and is responsible for the emergence of the short-distance regime $d \ll \lambda_\mathrm{SPP}$ where the Casimir force $\sim 1/d^3$ [19]. At large distances, a finite Ω leads to a small correction to the well-known Casimir force $\sim 1/d^4$ between perfect conductors [2, 9, 10].

V. CONCLUSION

We have pointed out that the Casimir attraction between realistic materials can be quantitatively understood, at short distances, in terms of the interaction between electromagnetic surface plasmon (or phonon) polaritons. The modes overlap across the vacuum gap and split into symmetric and antisymmetric combinations which contribute with different signs to the Maxwell stress tensor and hence to the Casimir force. We discussed in particular the short-distance regime of the Casimir force where $F = H/d^3$ and have given an analytical formula for the Hamaker constant H. We recover previous results for nonabsorbing materials and evaluate a correction due to absorption. Our results have been validated by comparing to a numerical calculation based on Lifshitz theory.

The approach presented here has the advantage of linking in a transparent way the Casimir force to the actual physical properties of the material surface. This suggests the possibility of engineering the surface plasmon polariton dispersion relation to modify the Casimir force. Indeed, as it has been shown, the Casimir force at short distances is entirely due to the interaction between surface polaritons. Magnetic materials which exhibit Casimir repulsion [37] and support s-polarized surface waves when Re $\mu < -1$ [38] are good candidates. The folding of the dispersion relation in reciprocal space by a grating, known to change the surface wave behaviour [39] could also lead to a substantial modification of the Casimir force.

Acknowledgments. — This work has been supported by the bilateral French-German programme "Procope" under project numbers 03199RH and D/0031079.

APPENDIX A: ANGULAR SPECTRUM ANALYSIS

In this appendix, we compute the Casimir force in terms of an angular spectrum representation of the electromagnetic fields that is adapted to the planar geometry at hand.

Letting the vacuum gap occupy the region $-d < z < 0$, we can expand the electric field in the gap as

$$\mathbf{E}(\mathbf{x},\omega) = \sum_{\mu=\mathrm{s,\,p}} \int d^2K \, \left(E^\mu_-(\mathbf{K})\, \mathrm{e}^{-ik_z z} \mathbf{e}^-_\mu + E^\mu_+(\mathbf{K})\, \mathrm{e}^{ik_z(z+d)} \mathbf{e}^+_\mu \right) \mathrm{e}^{i\mathbf{K}\cdot\mathbf{X}} \qquad \text{(A1)}$$

where $\mathbf{K} = (k_x, k_y)$ is the component of the wavevector parallel to the interfaces and $k_z = \sqrt{(\omega/c)^2 - K^2}$ its perpendicular component. The $\mathbf{e}^\pm_\mu$ ($\mu =$ s, p) are unit polarization vectors, and $E^\mu_\pm(\mathbf{K})$ are the amplitudes of up- and downwards propagating plane waves. A similar expansion holds for the magnetic field $\mathbf{H}(\mathbf{x},\omega)$ with amplitudes $H^\mu_\pm(\mathbf{K})$. We get the averaged Maxwell stress tensor by integrating incoherently over the contributions $T^\mu_{zz}(\mathbf{K})$ of individual modes. For the particular case of a p-polarized evanescent mode ($K > \omega$), we get by straightforward algebra

$$T^{\mathrm{p}}_{zz}(\mathbf{K}) = 2\mu_0 v^2 \,\mathrm{Re}\left[H^{\mathrm{p}*}_+(\mathbf{K}) H^{\mathrm{p}}_-(\mathbf{K}) \right]. \qquad \text{(A2)}$$

The up- and downward propagating amplitudes are of course related via the reflection coefficient from the upper interface. Taking the phase references in Eq. (A1) into account, we have

$$H^{\mathrm{p}}_- = r_{\mathrm{p}}\, \mathrm{e}^{ik_z d} H^{\mathrm{p}}_+ = r_{\mathrm{p}}\, \mathrm{e}^{-\omega v d/c} H^{\mathrm{p}}_+ \approx \pm H^{\mathrm{p}}_+, \qquad \text{(A3)}$$

where the last equality applies in the vicinity of the coupled surface resonances defined by Eq. (5). The condition $r_{\mathrm{p}}\, \mathrm{e}^{-\omega v d/c} = +1$ thus corresponds to a symmetric magnetic field distribution on both interfaces, because $H^{\mathrm{p}}_+ = H^{\mathrm{p}}_-$. In addition, with our sign convention, this mode gives an attractive contribution proportional to $+|H^{\mathrm{p}}_-|^2$ to the stress tensor (A2). The opposite is true for antisymmetric modes.

The sign of the Casimir force due to the coupled polariton modes can also be understood in terms of the charge densities excited on the surfaces, as pointed out by Gerlach [21]. These can be found from the normal component of the electric field. For a symmetric mode, we get surface charges with opposite sign, hence an attractive force, while an antisymmetric mode corresponds to equal surface charges.

[1] H. B. G. Casimir, Proc. Koninkl. Ned. Akad. Wetenschap. **51**, 793 (1948)
[2] J. Schwinger, J. Lester L. DeRaad and K. A. Milton, Ann. Phys. (N.Y.) **115**, 1 (1978).
[3] G. Plunien, B. Müller and W. Greiner, Phys. Rep. **134**, 87 (1986)
[4] M. Bordag, U. Mohideen and V. M. Mostepanenko, Phys. Rep. **353**, 1(2001)
[5] S. K. Lamoreaux, Am. J. Phys. **67**, 850 (1999)
[6] S. K. Lamoreaux, Phys. Rev. Lett. **78**, 5 (1997)
[7] U. Mohideen and A. Roy, Phys. Rev. Lett. **81**, 4549 (1998)
[8] G. L. Klimchitskaya, A. Roy, U. Mohideen, and V.M. Mostepanenko, Phys. Rev. A **60**, 3487 (1999)
[9] G. L. Klimchitskaya, U. Mohideen, and V. M. Mostepanenko, Phys. Rev. A **61**, 062107 (2000)
[10] A. Lambrecht and S. Reynaud, Eur. Phys. J. D **8**, 309 (2000)
[11] C. Genet, A. Lambrecht and S. Reynaud, Phys. Rev. A **62**, 012110 (2000)
[12] R. Tadmor, J. Phys.: Condens. Matt. **13**, L195 (2001)
[13] C. Genet, A. Lambrecht, P. Maia Neto and S. Reynaud, Europhys. Lett. **62**, 484 (2003)
[14] H. B. Chan, V. A. Aksyuk, R. N. Kleiman, D. J. Bishop and F. Capasso, Phys. Rev. Lett. **87**, 211801 (2001)
[15] H. B. Chan, V. A. Aksyuk, R. N. Kleiman, D. J. Bishop and F. Capasso, Science **291**, 1941 (2001)
[16] E. Buks and M. L. Roukes, Phys. Rev. B **63**, 033402 (2001)
[17] P. W. Milloni, *The Quantum Vacuum: An Introduction to Quantum Electrodynamics* (Academic Press, London, 1994)
[18] V. M. Mostepanenko and N. N. Trunov, *The Casimir Effect and Its Applications* (Oxford Science Publications, Oxford, 1997)
[19] E. M. Lifshitz, Soviet Phys. JETP **2**, 73 (1956) [J. Exper. Theoret. Phys. USSR **29**, 94 (1955)]

[20] N. G. Van Kampen, B. R. A. Nijboer and K. Schram, Phys. Lett. A **26**, 307 (1968)

[21] E. Gerlach, Phys. Rev. B **4**, 393 (1971)

[22] C. Genet, A. Lambrecht and S. Reynaud, preprint quant-ph/0302072 (2003)

[23] E.D. Palik, *Handbook of Optical constants of Solids*, (Academic Press, San Diego, 1991)

[24] S. M. Rytov, Yu. A. Kravtsov and V. I. Tatarskii, *Elements of Random Fields*, vol. 3 of *Principles of Statistical Radiophysics* (Springer, Berlin, 1989)

[25] L. Knöll, S. Scheel and D.-G. Welsch, *QED in Dispersing and Absorbing Media*, in *Coherence and Statistics of Photons and Atoms*, edited by J. Perina (John Wiley & Sons, Inc., New York, 2001)

[26] C. Raabe, L. Knöll, and D.-G. Welsch, Phys. Rev. A 68 (2003) 033810. Note that Eq. (82) in this paper is based on an inaccurate evaluation of the integral Eq. (E9). Once this is corrected, we find agreement with Eq. (12) reported here.

[27] C. Henkel, K. Joulain, J.-Ph. Mulet and J.-J. Greffet, J. Opt. A: Pure Appl. Opt. **4**, S109 (2002)

[28] L. H. Ford, Phys. Rev. D **38**, 528 (1988)

[29] L. H. Ford, Phys. Rev. A **48**, 2962 (1993)

[30] H. Raether, *Surface Plasmons on Smooth and Rough Surfaces and on Gratings* (Springer, Berlin, 1988)

[31] A.V. Shchegrov, K. Joulain, R. Carminati and J.-J. Greffet, Phys. Rev. Lett, **85**, 1548 (2000)

[32] K. Joulain, R. Carminati, J.-Ph. Mulet, and J.-J. Greffet, Phys. Rev. B (2003), in press; e-print physics/0307018.

[33] D. Marcuse, *Theory of Dielectric Optical Waveguides*, 2nd ed. (Academic Press, San Diego, 1991)

[34] A. Krishnan, T. Thio, T. J. Kim, H. J. Lezec, T. W. Ebbesen, P. A. Wolff, J. Pendry, L. Martin-Moreno and F. J. Garcia-Vidal, Opt. Commun. **200**, 1 (2001)

[35] A. Messiah, *Mécanique quantique*, vol. 1, new ed. (Dunod, Paris, 1995).

[36] The numerical integration uses the Lifshitz formula and proceeds along the imaginary frequency axis $\omega = \mathrm{i}\xi$. The dielectric function $\varepsilon(\mathrm{i}\xi)$ is constructed from the tabulated data at real frequencies using the sum rules given in [9, 10].

[37] O. Kenneth, I. Klich, A. Mann and M. Revzen, Phys. Rev. Lett. **89**, 033001 (2002)

[38] R. Ruppin, Phys. Lett. A **277**, 61 (2000)

[39] J.-J. Greffet, R. Carminati, K. Joulain, J.-Ph. Mulet, S. Mainguy, and Y. Chen, Nature, **416**, 61 (2002)